An Experimental Study on Maneuvering Hydrodynamic Forces in Shallow Water

Masayoshi HIRANO, *Member*, Junshi TAKASHINA, *Member*,
Shuko MORIYA, *Member* and Yoshiaki NAKAMURA

西 部 造 船 会 会 報
第 69 号 別 刷
昭 和 60 年 3 月

Reprinted from
TRANSACTIONS
OF
THE WEST-JAPAN SOCIETY OF
NAVAL ARCHITECTS
No. 69 MARCH 1985

(昭和59年11月西部造船会第69回例会において講演)

An Experimental Study on Maneuvering Hydrodynamic Forces in Shallow Water

Masayoshi HIRANO*, *Member*, Junshi TAKASHINA*, *Member*,
Shuko MORIYA*, *Member* and Yoshiaki NAKAMURA*

Summary

This paper presents experimental results on the maneuvering hydrodynamic forces in shallow water with some theoretical considerations. Force measurement tests by means of a PMM were performed with use of three kinds of ship models at various water depths. The experimental results show general features of the shallow water effects on the maneuvering hydrodynamic forces including hull forces and rudder forces. Theoretical studies were also made to examine the shallow water effects on the hydrodynamic derivatives of hull and on the hydrodynamic interaction between hull and rudder. Furthermore, with aid of theoretical studies, practical formulae for estimating the linear hydrodynamic derivatives in shallow water were developed.

1. Introduction

Significance of the navigation safety in restricted water area such as ports and waterways has greatly increased in recent years because of the growth in ship sizes and the diversification in ship types. Among many factors, which characterize the ship maneuverability in restricted water area, the shallow water effects on the hydrodynamic forces may be one of the most important points because of significant changes in the maneuvering characteristics caused by them. Many studies have been made on the maneuvering hydrodynamic forces in shallow water from both theoretical and experimental aspects[1)~6)], but there still remain a great many problems to be solved or to be clarified.

In this context, the authors recently made an attempt to investigate the shallow water effects on the maneuvering hydrodynamic forces mainly from experimental aspects. Using three kinds of ship models (three different hull forms), measurement tests of the maneuvering hydrodynamic forces both in deep water and in shallow water were performed. In the model tests, hull forces together with rudder forces were measured with a PMM test device, and test results were analyzed as functions of water depth. In addition, a study from theoretical point of view was made, that is, experimental results were reviewed with applications of existing theories. This paper describes results obtained by these investigations for the shallow water effects on the maneuvering hydrodynamic forces.

2. Model Description

Three kinds of ship models, namely three typical hull forms of a tanker (ESSO OSAKA), a LNGC and a PCC, were tested in the present study in order to investigate the shallow water effects on the maneuvering hydrodynamic forces in connection with ship hull particulars. These models are 2.5 m long and wooden ones, and the principal particulars of hull of these models are given in Table 1. Moreover the principal particulars of rudder and propeller are also given in

* Akishima Laboratory, Mitsui Engineering and Shipbuilding Co., Ltd.

Table 1 Principal Particulars of Models

	TANKER	LNGC	PCC
L (m)	2.500	2.500	2.500
B (m)	0.408	0.415	0.482
d (m)	0.167	0.100	0.134
∇ (m^3)	0.141	0.072	0.084
D_p (m)	0.070	0.075	
P/D_p	0.715	0.600	
A_R/Ld	1/58.5	1/44.5	

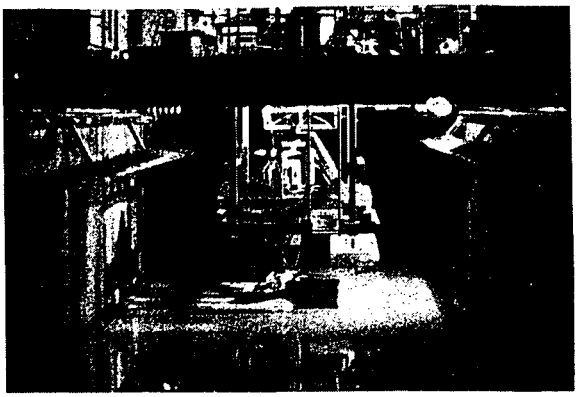

Photo 1 PMM Test in Shallow Water

Table 1 for the tanker and the LNGC models, for which rudder forces were measured together with hull forces.

3. Contents of Model Experiments

The model experiments of the present study were carried out at the small towing tank of Akishima Laboratory, Mitsui Engineering and Shipbuilding Co., Ltd.. Principal dimensions of the tank are: length × breadth × water depth = 100 m × 5 m × 2.15~0 m. The shallow water was made by lowering water level of the tank. The force measurement tests were performed with a conventional PMM test device with maximum sway amplitude of 600 mm. In the shallow water test, the PMM test device was set on the shallow water frame installed on the towing carriage as shown in Photo 1.

Contents of the force measurement tests are described in the following.

(1) Hull forces: Static mode tests

Static drift angle tests were performed for the three kinds of ship models at the following water depth conditions where H/d denotes the ratio of water depth to ship draft.

Tanker: $H/d=\infty$, 1.5, 1.2
LNGC : $H/d=\infty$, 3.0, 2.0, 1.5, 1.3, 1.2
PCC : $H/d=\infty$, 3.0, 2.0, 1.5, 1.3, 1.2.

The tests were performed for ship models of bare hull condition without propeller and rudder. The ship models were towed with an advance speed of $U=0.45$ m/sec ($Fn=0.091$), giving a drift angle in a range of $\beta=0°\sim15°$.

(2) Hull forces: Dynamic mode tests

Pure yaw tests were performed for the tanker and the LNGC models at the following water depth conditions.

Tanker: $H/d=\infty$, 1.5, 1.2
LNGC : $H/d=\infty$, 2.0, 1.5, 1.2.

In the same manner as the static mode tests, the tests were performed for bare hull condition with an advance speed of $U=0.45$ m/sec. Yaw rate amplitude was varied in a range of $\bar{r}'=0.2\sim0.8$.

(3) Rudder force tests

Rudder force measurements at behind-hull condition were made for the tanker and the LNGC models at the following water depth conditions.

Tanker: $H/d=\infty$, 1.5, 1.2
LNGC : $H/d=\infty$, 1.5, 1.2.

Rudder forces were measured by taking rudder with angle of $\delta=-20°\sim20°$. In the rudder force tests at straight towed condition ($\beta=0°$) with an advance speed of $U=0.45$ m/sec, propeller load was varied by changing propeller revolution speed. The tests at obliquely towed condition ($\beta=-20°\sim20°$) with $U=0.45$ m/sec were made at the model self-propulsion point, and advance coefficients Js, defined as $Js=U/(nD)$ (n : propeller revolution speed, D: propeller diameter), at the model self-propulsion point are as follows at each water depth conditions of $H/d=\infty$, 1.5 and 1.2.

Tanker: $Js=0.47$, 0.42, 0.40
LNGC : $Js=0.59$, 0.53, 0.48.

4. Experimental Results

4.1 Hull Forces

Hull force analyses in this paper were made by introducing dimensionless forms of

$$Y'_H=\frac{Y_H}{\frac{1}{2}\rho LdU^2},\quad N'_H=\frac{N_H}{\frac{1}{2}\rho L^2dU^2} \tag{1}$$

where Y_H : hull lateral force
N_H : hull yaw moment about midship
ρ : water density
L : ship length between perpendiculars
d : ship draft
U : ship speed.

Results of the static drift angle tests were analyzed by employing the following second order polynomials with respect to dimensionless sway velocity $v'(=v/U=-\sin\beta)$.

$$\begin{aligned} Y'_H&=Y'_vv'+Y'_{v|v|}v'|v'| \\ N'_H&=N'_vv'+N'_{v|v|}v'|v'| \end{aligned} \tag{2}$$

Figs. 1 and 2 show experimental results of the linear static derivatives Y'_v and N'_v respectively

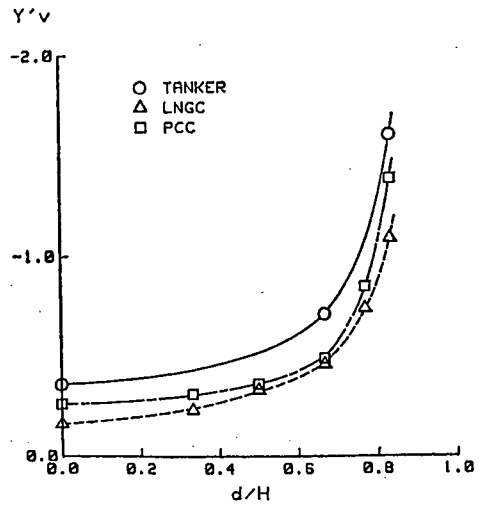

Fig. 1 Linear Static Derivative Y'_v as a Function of Draft-to-Depth Ratio

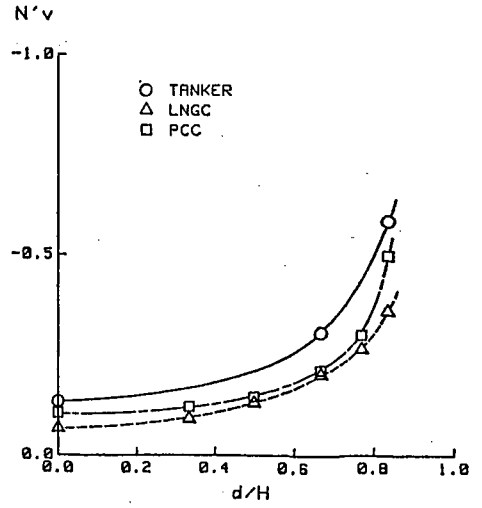

Fig. 2 Linear Static Derivative N'_v as a Function of Draft-to-Depth Ratio

which were obtained by expressing measured lateral force and yaw moment with Eq. (2), where the ratio of ship draft to water depth d/H is taken in abscissa. Remarkable shallow water effects on both $Y'v$ and $N'v$ can be seen for all of the three kinds of ship models.

Results of the pure yaw tests were analyzed with the following second order polynomials with respect to dimensionless yaw rate $r'(=rL/U)$, where the inphase component forces were considered.

$$\begin{aligned} Y'_H &= Y'_r r' + Y'_{r|r|} r'|r'| \\ N'_H &= N'_r r' + N'_{r|r|} r'|r'| \ . \end{aligned} \tag{3}$$

Figs. 3 and 4 show experimental results of the linear rotary derivatives Y'_r and N'_r respectively which are based on the expressions in Eq. (3). In determination of Y'_r, appropriate values of m'_x (added inertia force in x-direction) based on the results described in References 5), 6) and 4) were assumed, because measurement tests for m'_x were not performed in the present study. The shallow water effects on the linear rotary derivatives may be not so conspicuous as those on the linear static derivatives.

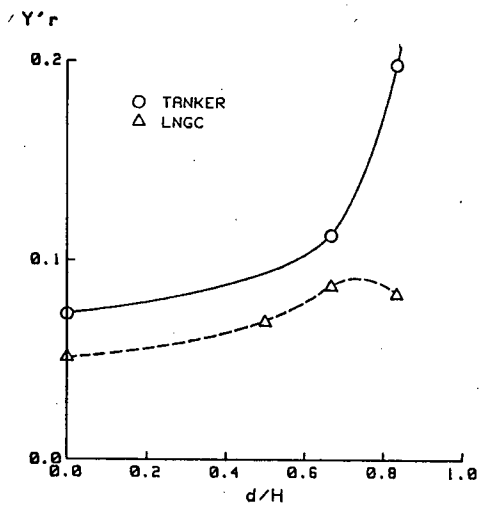

Fig. 3 Linear Rotary Derivative Y'_r as a Function of Draft-to-Depth Ratio

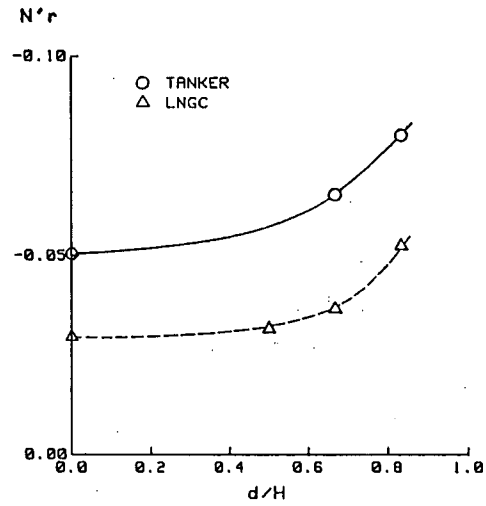

Fig. 4 Linear Rotary Derivative N'_r as a Function of Draft-to-Depth Ratio

4.2 Rudder Forces

In general rudder forces including hydrodynamic force and moment induced on ship hull by rudder action can be written in the following form[7].

$$\begin{aligned} Y_R &= (1+a_H)F_N \cos\delta \\ N_R &= (x_R + a_H x'_H L)F_N \cos\delta \end{aligned} \tag{4}$$

where Y_R : rudder lateral force
N_R : rudder yaw moment about midship
F_N : rudder normal force
δ : rudder angle
x_R : x-coordinate of rudder position.

In Eq. (4), a_H and x'_H denote the force and the moment coefficients due to the rudder-to-hull interaction respectively. The shallow water effects on a_H and x'_H are examined with results obtained by the rudder force tests at straight towed condition. Figs. 5 and 6 show results of a_H and x'_H respectively at the model self-propulsion point for both the tanker and the LNGC mod-

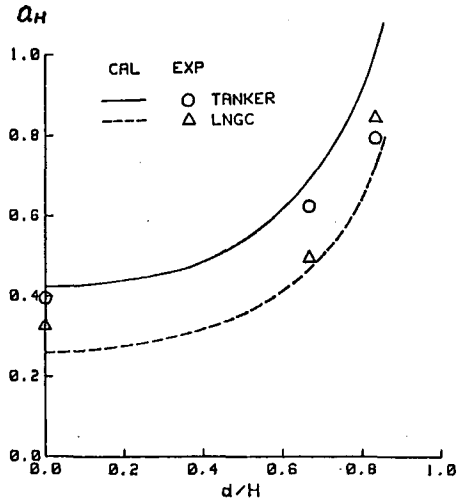

Fig. 5 Force Coefficient of Rudder-to-Hull Interaction as a Function of Draft-to-Depth Ratio

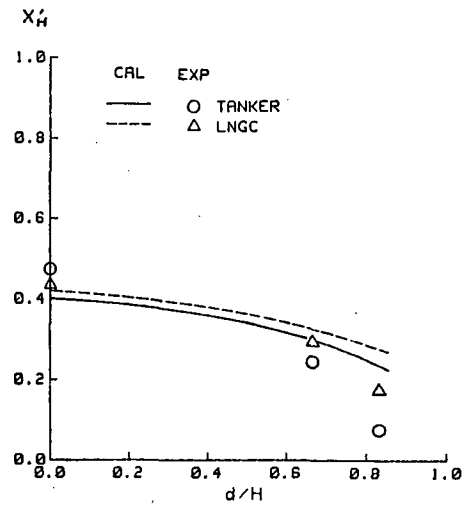

Fig. 6 Moment Coefficient of Rudder-to-Hull Interaction as a Function of Draft-to-Depth Ratio

els. Considerable increase in a_H in shallow water can be seen in Fig. 5. As water depth decreases, x'_H decreases as shown in Fig. 6. This means that the point on which the rudder-to-hull interaction force acts moves forward in shallow water.

Effective inflow velocity into rudder, u_R, can be obtained from rudder normal force measured at behind-hull condition with a concept of the rudder normal force identity on a basis of the open water performance of rudder. The shallow water effects on the effective rudder inflow velocity, obtained with this concept from results of the rudder force tests at straight towed condition, were examined in connection with propeller load effects. Fig. 7 shows results of the tanker model, where dimensionless effective rudder inflow velocity u_R/U is employed in ordinate and advance coefficient J_S is employed in abscissa as an index of the propeller load. In the higher propeller load region, no distinct shallow water effects on u_R/U may be seen. However, as propeller load becomes lower (J_S becomes larger), difference in u_R/U due to water depth change becomes clear. This may be attributed to the fact that the effective wake fraction at rudder position increases in shallow water[5].

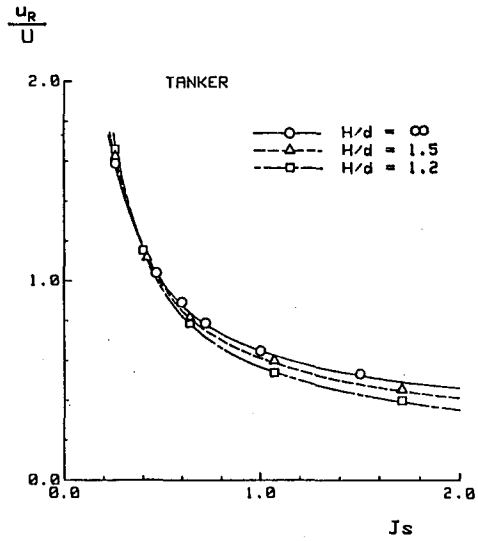

Fig. 7 Effective Rudder Inflow Velocity for Three Different Water Depths

Effective inflow angle into rudder can be estimated on a basis of the rudder angle of zero normal force, δ_R. Introducing a concept of the flow-rectification coefficient γ_R, the following expression can be written with respect to δ_R for the condition of obliquely towing.

$$\delta_R \frac{u_R}{U} = \gamma_R \beta + \frac{v_{RP}}{U} \tag{5}$$

where the second term in the right-hand side means the offset rudder angle due to asymmetry of propeller slip-stream. Characteristics of $\delta_R u_R/U$ versus β were analyzed with results obtained by the rudder force tests at obliquely towed condition. Fig. 8 shows results at the model self-

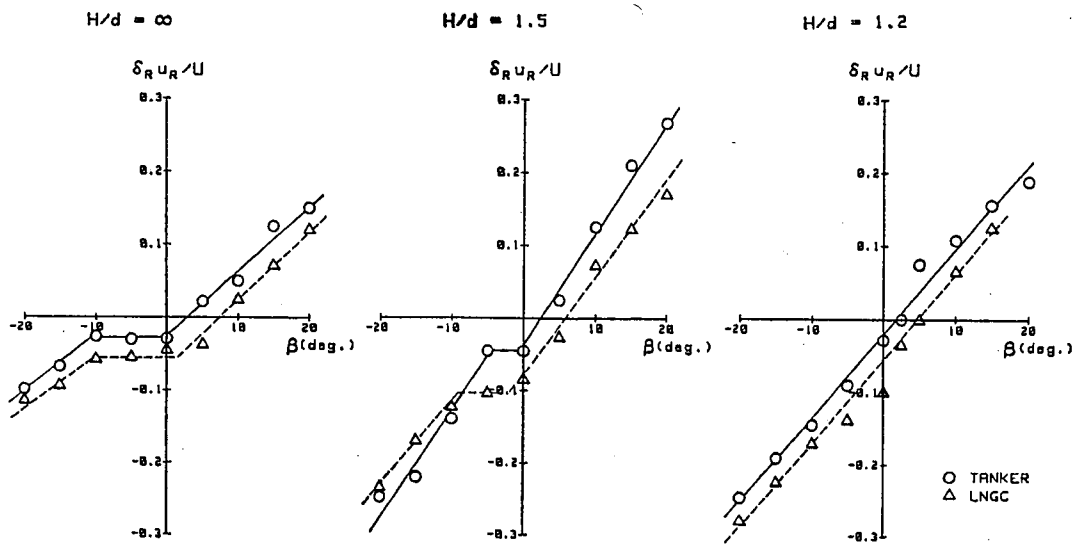

Fig. 8 Effective Rudder Inflow Angle for Three Different Water Depths

propulsion point for both the tanker and the LNGC models. Similar tendency regarding the shallow water effects on the $\delta_R u_R/U$ versus β characteristics can be seen for both ship models. The flow-rectification coefficient γ_R, which can be defined as a slope in $\delta_R u_R/U$ versus β characteristics as is self-evident from Eq. (5), increases in shallow water. But changes in γ_R due to water depth decrease may not necessarily be monotonous.

5. Discussions

5.1 Hull Forces

The maneuvering hydrodynamic forces in shallow water can be calculated with making use of low aspect ratio wing theories, and some available results have already been reported[2)3)]. In the present study, a simplified theory for the linear static derivatives was developed first, details of which are described in Appendix. Then by utilizing this simplified theory, a study was made on estimate formulae for the linear derivatives in shallow water. In the present theory, flow around ship hull is represented with a simple lifting surface model, which consists of a single horse-shoe vortex starting from the 1/4 chord length behind the leading edge and its infinite series of images with respect to the free surface and the bottom surface.

According to Appendix, namely from Eq. (A 7)

$$Y'_v = -\pi \cdot \frac{k}{\frac{d}{2H}k + \frac{\pi d}{2H}\cot\frac{\pi d}{2H}} \,. \tag{6}$$

Examining values of Y'_v in Eq. (6) at two extreme conditions, that is, in deep water $(H/d=\infty)$ and at zero under-keel clearance condition $(H/d=1.0)$, then

$$\begin{aligned} Y'_v &= -\pi k \quad \text{at} \quad H/d=\infty \\ Y'_v &= -2\pi \quad \text{at} \quad H/d=1.0\,. \end{aligned} \tag{7}$$

This suggests that Eq. (6) can be interpreted as an expression in which the aspect ratio of a ship, $k(=2d/L)$, apparently varies from deep water to shallow water as

$$k \to \frac{k}{\frac{d}{2H}k + \frac{\pi d}{2H}\cot\frac{\pi d}{2H}} \,. \tag{8}$$

Then a concept of "effective aspect ratio in shallow water" k_e may be introduced, which is de-

fined with an experimental constant λ as

$$k_e = \frac{k}{\frac{d}{2H}k + \left(\frac{\pi d}{2H}\cot\frac{\pi d}{2H}\right)^{\lambda}}, \tag{9}$$

and this was derived from somewhat intuitive insight.

By utilizing this concept of the effective aspect ratio in shallow water, an attempt was made to extend applicability of the well-established estimate formulae for the linear derivatives in deep water[8)9)], to shallow water region. Estimate formulae for the linear static derivatives in shallow water may be written in the following form with k_e on a basis of those in deep water.

$$Y'_v = -\frac{\pi}{2}k_e - 1.4\,C_B \cdot B/L \tag{10}$$

$$N'_v = -k_e\,. \tag{11}$$

It is needless to say that Eqs. (10) and (11) can cover estimations of the deep water derivatives. Experimental results for Y'_v and N'_v are shown in Figs. 9 and 10 respectively with marks such as empty circles, where k_e is taken in abscissa. Estimated results with Eqs. (10) and (11) are also shown in Figs. 9 and 10 respectively with solid lines, where $C_B \cdot B/L = 0.10$ is supposed for Y'_v estimation. Experimental constants of $\lambda = 2.3$ and 1.7 are employed in estimations of Y'_v and N'_v respectively, which are determined so that the estimations with Eqs. (10) and (11) can fit well the experimental results. The results shown in Figs. 9 and 10 indicate that, by employing appropriate experimental constants, the estimate formulae of Eqs. (10) and (11) based on a concept of the effective aspect ratio in shallow water could give fairly good estimation to the linear static derivatives in shallow water.

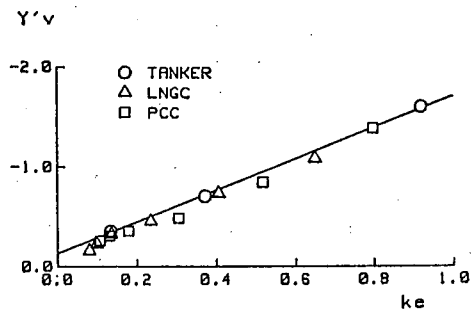

Fig. 9 Linear Static Derivative Y'_v as a Function of Effective Aspect Ratio

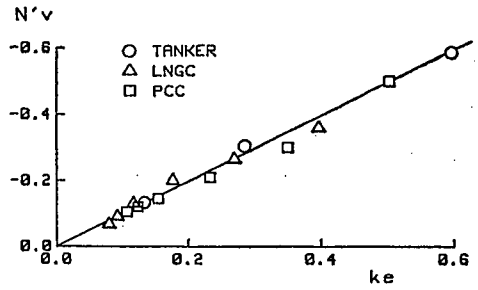

Fig. 10 Linear Static Derivative N'_v as a Function of Effective Aspect Ratio

In applying the concept of k_e to the rotary derivatives, there could arise problems because it is basically impossible to represent flow around ship hull in turning motion with a single horse-shoe vortex. However, in this paper, the same attempt as those for the linear static derivatives was made for the linear rotary derivatives, assuming that Eq. (9) could be a kind of empirical formula. Then estimate formulae for the linear rotary derivatives in shallow water can be written in the following form.

$$Y'_r = \frac{1}{4}\pi k_e \tag{12}$$

$$N'_r = -0.54k_e + k_e^2\,. \tag{13}$$

Figs. 11 and 12 show experimental results for Y'_r and N'_r together with estimated ones by Eqs. (12) and (13) respectively, where experimental constant of $\lambda = 0.7$ is employed in the esti-

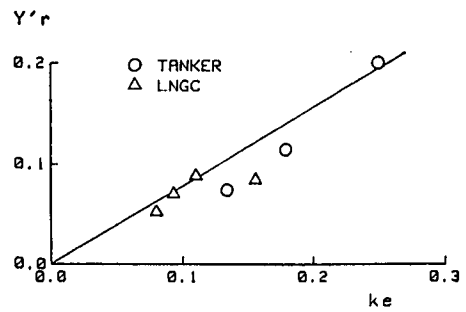

Fig. 11 Linear Rotary Derivative Y'_r as a Function of Effective Aspect Ratio

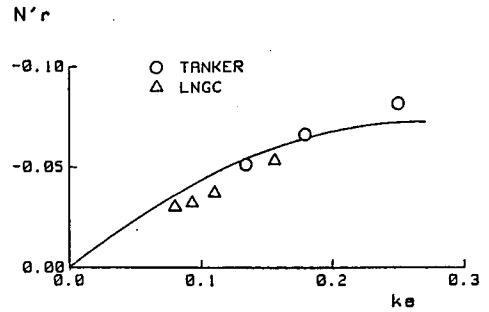

Fig. 12 Linear Rotary Derivative N'_r as a Function of Effective Aspect Ratio

mations of both Y'_r and N'_r. It may be seen in Figs. 11 and 12 that, by employing appropriate experimental constants in the same manner as those for the linear static derivatives, the estimate fomrulae in Eqs. (12) and (13) also could give satisfactory estimation to the linear rotary derivatives. It may be mentioned from the matters discussed above that the estimate formulae developed on a basis of those in deep water with a concept of the effective aspect ratio in shallow water, Eqs. (10)～(13), could be very useful for practical estimations of the linear derivatives in shallow water.

5.2 Rudder-to-Hull Interaction Forces

The hydrodynamic forces induced on ship hull by rudder action can be calculated by solving interaction problems between two wings which are located fore and aft each other. In the present study, calculations of a_H and x'_H were made with a theory for the interaction forces in shallow water, which was developed for shallow water in the same manner as that in Reference 10) on a basis of the theory previously developed by the authors for the deep water interaction forces[11]. Computed results with this theory for a_H and x'_H are shown in Figs. 5 and 6 respectively together with experimental results. Computations were made under the following conditions.

Number of strips in spanwise : 1 for ship hull and 3 for rudder
Number of terms in Glauert's mode function : 9 for both ship hull and rudder
Number of images : 40 at $H/d=1.2$ (as an example).

It may be seen in Figs. 5 and 6 that the computed results explain well the shallow water effects on both a_H and x'_H obtained by model experiments in qualitative aspects.

6. Concluding Remarks

A study on the maneuvering hydrodynamic forces in shallow water was made mainly from experimental aspects. Using three typical hull forms of ship models, hull forces together with rudder forces were measured both in deep water and in shallow water, and test rusults were analyzed as functions of water depth. In addition, experimental results were reviewed from theoretical point of view with applications of existing theories.

The main conclusions of the present study are summarized as follows.

(1) General features of the shallow water effects on the linear hydrodynamic derivatives are shown on a basis of results obtained by the hull force tests.

(2) General features of the shallow water effects on the rudder-to-hull interaction forces, the effective rudder inflow velocity and the effective rudder inflow angle are also shown on a basis of experimental results obtained by the rudder force tests.

(3) Estimate formulae for the linear derivatives of hull forces in shallow water were developed for practical use, by introducing a concept of the effective aspect ratio in shallow water, based on the well-established estimate formulae for deep water linear derivatives. And its validity was confirmed by comparing estimated results with experimental ones.

As stated in Introduction, there are a great many problems to be solved or to be clarified in the area of the maneuvering hydrodynamic forces in shallow water. It is really expected that much more efforts will be devoted to this area in future.

Acknowledgements

A part of the present study was carried out as a cooperative research work in the working group of Japan Towing Tank Conference, named as Japan Maneuverability Prediction (JAMP), under the leadership of Dr. H. Fujii. The authors would like to express their thanks to all of the JAMP members for their useful discussions and suggestions.

References

1) Fujino, M.: Maneuverability in Restricted Waters, State of the Arts, University of Michigan, Department of Naval Architecture and Marine Engineering, Report 184 (1976)
2) Inoue, S. and Murayama, K.: Calculation of Turning Ship Derivatives in Shallow Water (in Japanese), Transactions of the West-Japan Society of Naval Architects, Vol. 37 (1969)
3) Sundstrom, O.: Measurements of Side Forces and Moments on a Ship Model and a Comparison with Simplified Theories, The Royal Institute of Technology in Stockholm (1978)
4) Pettersen, B.: Calculation of Potential Flow about Ship Hulls in Shallow Water with Particular Application to Maneuvering, Dr. Thesis, The Norwegian Institute of Technology (1980)
5) Fujino, M. and Ishiguro, T.: A Study on Mathematical Model Describing Manoeuvring Motions in Shallow Water (in Japanese), Journal of the Society of Naval Architects of Japan, Vol. 156 (1984)
6) Kijima, K., Murakami, M., Katsuno, T. and Nakiri, Y.: A Study on the Ship Maneuvering Characteristics in Shallow Water (in Japanese), Transactions of the West-Japan Society of Naval Architects, Vol. 69 (1985)
7) Kose, K.: On a New Mathematical Model of Maneuvering Motions of a Ship and Its Applications, International Shipbuilding Progress, Vol. 29, No. 336 (1982)
8) Inoue, S., Hirano, M. and Kijima, K.: Hydrodynamic Derivatives on Ship Manoeuvring, International Shipbuilding Progress, Vol. 28, No. 321 (1981)
9) Inoue, S., Hirano, M., Hirakawa, Y. and Mukai, K.: The Hydrodynamic Derivatives on Ship Maneuverability in Even Keel Condition (in Japanese), Transactions of the West-Japan Society of Naval Architects, Vol. 57 (1979)
10) Fujino, M., Kano, T. and Motora, S.: A Fundamental Study on Ship's Hull to Rudder Interaction (2nd Report) (in Japanese), Journal of the Society of Naval Architects of Japan, Vol. 147 (1980)
11) Hirano, M., Takashina, J., Moriya, S. and Fukushima, M.: Open Water Performance of Semi-balanced Rudder, Transactions of the West-Japan Society of Naval Architects, Vol. 64 (1982)

Appendix A Simplified Theory for Linear Static Derivatives in Shallow Water

In the present study, it is assumed that flow around ship hull moving in shallow water with a small angle of attack can be modeled by bound vortices and trailing vortices on a flat plate with its infinite series of images with respect to the free surface and the bottom surface as shown in Fig. A 1. Based on linear approximation of the low aspect ratio wing theory in which the bound vortex strength $\gamma(\xi)$ is constant across the span and the trailing vortex is parallel to the x-axis, the normal induced velocity $w(x)$ at a point $P(x, 0, 0)$ due to both the bound vorti-

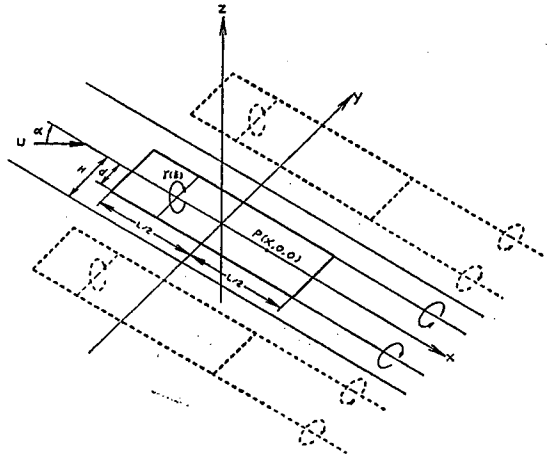

Fig. A1 Coordinate System and Flow Model

ces and the trailing vortices can be expressed by the following equations.

$$w(x)=-\frac{1}{2\pi}\int_{-L/2}^{L/2}\frac{\gamma(\xi)}{x-\xi}K(x,\xi)d\xi \tag{A1}$$

$$K(x,\xi)=\frac{1}{2}\left\{\sum_{n=-\infty}^{\infty}\left(\frac{x-\xi+\sqrt{(d-2nH)^2+(x-\xi)^2}}{d-2nH}+\frac{x-\xi+\sqrt{(d+2nH)^2+(x-\xi)^2}}{d+2nH}\right)\right\}. \tag{A2}$$

The kernel function $K(x,\xi)$ is transformed into the following form according to Sundstrom[3].

$$K(x,\xi)=\frac{2\pi}{H}(x-\xi+|x-\xi|)\cot\frac{\pi d}{2H}+\frac{2}{\pi}\int_0^{\pi/2}d\theta\sin\theta\tan^{-1}\left(\tan\frac{\pi d}{2H}\cdot\coth\frac{\pi|x-\xi|}{2H\sin\theta}\right). \tag{A3}$$

Alternative expressions of Eqs. (A 1) and (A 3) with using nondimensional expressions of $x'=2x/L$, $\xi'=2\xi/L$, $k=2d/L$ and $\mu=\pi d/2H$ are given in the form

$$w(x')=-\frac{1}{2\pi}\int_{-1}^{1}\frac{\gamma(\xi')}{x'-\xi'}K(x',\xi')d\xi' \tag{A4}$$

$$K(x',\xi')=\frac{\mu\cot\mu}{k}(x'-\xi'+|x'-\xi'|)+\frac{2}{\pi}\int_0^{\pi/2}d\theta\sin\theta\tan^{-1}\left(\tan\mu\coth\frac{\mu|x'-\xi'|}{k\sin\theta}\right). \tag{A5}$$

For simplification, it is supposed that a single horse-shoe vortex starting from the 1/4 chord length behind the leading edge and its images represent the whole vortex system, and that vortex strength Γ is determined so that the boundary condition is satisfied at the point of the 3/4 chord length behind the leading edge.

Under this simplified flow model, Eqs. (A 4) and (A5) result in the following equation determining the vortex strength Γ.

$$-U\sin\alpha=-\frac{\Gamma}{2\pi}\left\{\frac{2\mu\cot\mu}{k}+\frac{2}{\pi}\int_0^{\pi/2}d\theta\sin\theta\tan^{-1}\left(\tan\mu\coth\frac{\mu}{k\sin\theta}\right)\right\}$$

$$\fallingdotseq-\frac{\Gamma}{2\pi}\left(\frac{2\mu\cot\mu}{k}+\frac{2}{\pi}\mu\right)\quad(\text{for}\quad k\ll1). \tag{A6}$$

Since the lifting force acting on the plate is calculated with $\rho U\Gamma$, the following simple expression for the linear static derivative Y'_v can be obtained.

$$Y'_v=-\frac{\rho U\Gamma}{\frac{1}{2}\rho\cdot2\cdot U^2\sin\alpha}=-\pi\cdot\frac{k}{\frac{d}{2H}k+\frac{\pi d}{2H}\cot\frac{\pi d}{2H}}. \tag{A7}$$